BULETINUL INSTITUTULUI POLITEHNIC DIN IAŞI
Publicat de
Universitatea Tehnică „Gheorghe Asachi” din Iaşi
Volumul 66 (70), Numărul 2, 2020
Secţia
CONSTRUCŢII DE MAŞINI

AN APPROACH ON SIMULATION OF SINE GEAR PROFILE USED ON CYLINDRICAL GEARS

BY

MIHĂIȚĂ HORODINCĂ*

"Gheorghe Asachi" Technical University of Iaşi, Romania,
Faculty of Machine Manufacturing and Industrial Management

Received: April 15, 2020
Accepted for publication: June 20, 2020

Abstract. Some theoretical approaches and computer aided simulations related with 2D sine gear profile on cylindrical gears are presented in this paper. Compared to a usual involute profile, the sine gear profile is a more convenient shape which mainly diminishes the sliding process, increases the load capacity and assures a smoother motion in gearing. Similarly with the generating method of involute profile of the flank faces on toothed wheel, the sine gear profile is obtained by pure rolling of a generating rack (having sine tooth profile) around a fixed pitch circle. The inner envelope bordered by the positions of generating rack during rolling describes the 2D sine gear profile. The main achievements of this paper are related with rolling simulation and 2D sine gear profiles detection in different circumstances. Some consequences related especially with the influence of generating rack shape (tooth addendum value) are also highlighted.

Keywords: sine gear profile; generating rack; rolling; simulation.

1. Introduction

The sine gear profile on cylindrical gears (Tkach *et al*., 2019; Hrytsay and Stupnytskyy, 2020) is a particular case of non-involute profiles. Here the

*Corresponding author: *e-mail*: horodinca@tuiasi.ro

generating rack (placed as cutting edge on a rack type cutter during manufacturing process with rolling) has a sine shape (with dedendum equal with addendum) which is relatively more complex than the generating rack used in gears with involute tooth profiles.

According with the literature, the sine gear profile on cylindrical gears, also known as cosine gear profile (Luo *et al.*, 2008; Hu and Wang, 2012; Laczik *et al.*, 2014; Wadagaonkar and Shinde, 2015; Lee, 2017; Lee, 2019; Si *et al*., 2020), has some significant advantages compared to the involute profile (regularly used). Firstly, the sliding process between the flanks faces of the toothed wheels involved in a gear is diminished (Tkach *et al.*, 2019), with two positive consequences: the power lost in heating phenomenon and the temperature decreases while the transmitted power in gear increases. Secondly, the tooth thickness on sine gear in the root area is bigger than the tooth thickness on involute profile; this means a lower tooth bending stress for the same loading or a higher loading capacity for the same bending stress as well (Wadagaonkar and Shinde, 2015). Thirdly, according with (Lee, 2017) the sine gear is appropriate to avoid the undercutting phenomenon which appears on involute gear profile (Alipiev *et al.*, 2013) for small number of teeth. Fourthly and last, the smoothness of the work (Wildhaber, 1966), the low level of noise, the absence of edge contact problem (Lee, 2019) is also an important feature of the sine gears.

The sine gear profile is applicable for many other types of external gears: face gears (Lee, 2019), bevel gears, non-circular bevel gears (Zheng *et al.*, 2016) and particularly for internal cylindrical gears (planetary gears) with small difference of number of teeth (Si *et al*., 2020) mainly because in certain conditions it is able to avoid the tooth tip interference.

This paper focuses on sine gear profile geometrical definition based on pure rolling simulation using a mathematical model and a method of detection for 2D sine gear profile (2D SGP) adapted from a previous work (Horodincă, 2020).

Similarly with involute tooth profile, the sine gear profile is the result of rolling between a movable sine shape generating rack (SSGR) which rolls on a fixed pitch circle (the datum line being permanently tangent to the pitch circle). The inner envelope bordered by all generating rack positions during rolling describes the 2D SGP. Some particularities of the 2D SGP are revealed.

2. A Mathematical Model of Sine Shape Generating Rack Position and Trajectory Used in Rolling Simulation

The significant characteristics of a SSGR used in rolling are revealed in Fig. 1. Mainly similar definitions and nomenclature as for involute gears (https://en.wikipedia.org/wiki/List_of_gear_nomenclature) can be used here. If consider the generating rack placed in a Cartesian coordinate system (CCS)

$x_1O_1y_1$ with the datum (pitch line) located on x_1-axis then any point P_{i1} placed on the generating rack should have mandatory the coordinates $x_1(P_{i1})$ and $y_1(P_{i1})$ in CCS $x_1O_1y_1$ interrelated by a sine function as follows:

$$y_1(P_{i1}) = h_a \cdot \sin[\frac{2 \cdot x_1(P_{(i1)})}{m}] \tag{1}$$

Here m is the gear module involved in definition of the circular pitch $p=\pi m$ (Fig. 1), t_t is the circular tooth thickness, s_t is the circular space thickness (here $t_t=s_t=p/2$), $h_a=c_h \cdot m$ is the addendum (equal with dedendum h_d), with $2 \cdot h_a$ the tooth depth, c_h being a proportionality factor (*e.g.* $c_h=1$). In Eq. (1) h_a is also the amplitude of the sine function. In the argument of a sine function involved in a harmonic motion $y(t)$ related by time t as ($y(t)=A \cdot \sin(\omega t)$) the angular velocity ω is related by period T with the relationship $\omega=2\pi/T$. In Eq. (1) the equivalent of t is $x_1(P_{i1})$ and the equivalent of $\omega=2\pi/T$ is $2/m$. From $2\pi/T=2/m$ results $T=\pi m$, this being exactly -as expected- the circular pitch $p=\pi m$ of SSGR and sine gear profile as well.

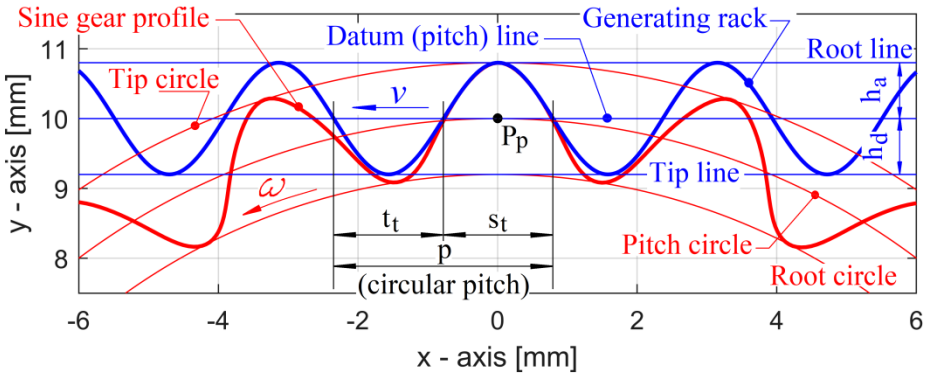

Fig. 1 – Sine gear profile and SSGR positions during rolling.

The rolling implies that the datum line should be tangent to pitch circle (having the radius $R_p=mZ/2$, with Z the number of teeth of the toothed wheel) in the pitch point P_p and consequently the tip line is tangent to root circle while the root line is tangent to tip circle. It is mandatory that the generating rack moves along its datum line with the velocity v strictly correlated with the rotation of pitch circle (around its centre) having the angular speed ω in order to avoid the sliding in the pitch point P_p, with the relationship $v=\omega R_p$ (as a gearing law). The 2D SGP is generated in a plane rigidly attached to the pitch circle.

A mathematical model of rolling for involute tooth profile generation was already exposed in a previous work (Horodincă, 2020). This model is fully available here if is adapted at SSGR. The parametric trajectory T_i of any point

P_{i1} placed on the SSGR during rolling (on fixed pitch circle) is described in a fixed CCS *xOy* by the equations:

$$x(P_i^{\beta}) = x_c + R_p \cos(\alpha - \beta) + [x(P_{i1}) - R_p\beta]\cos(\gamma) - [y(P_{i1})]\sin(\gamma) \quad (2)$$

$$y(P_i^{\beta}) = y_c + R_p \sin(\alpha - \beta) + [x(P_{i1}) - R_p\beta]\sin(\gamma) + [y(P_{i1})]\cos(\gamma) \quad (3)$$

Here $y_1(P_{i1})$ coordinates are mandatory described with Eq. (1). All other elements involved in Eqs. (2) and (3) are fully explained in (Horodincă, 2020).

A certain value of the parameter β (variable in a range between 0 and 2π) applied to all the points P_{i1} provides a full description of a single SSGR position (*i* is variable, β is constant) during rolling. The length of SSGR (or the number of teeth on SSGR as well) depends by $x_1(P_{i1})$ range in Eqs. (1), (2) and (3). Any two successive points P_i^{β} and P_{i+1}^{β} placed on this SSGR position are joined by a line segment. In CCS $x_1O_1y_1$ the abscissa $x_1(P_{(i+1)1})$ is expressed as $x_1(P_{(i+1)1}) = x_1(P_{i1}) + \Delta x$, with Δx small enough in order to have an accurate description of SSGR. The internal envelope bordered by all SSGR positions (during a completely rolling) is an approximation of the 2D SGP. The method of detection of this 2D SGP using a rotary ray (already depicted as an example in Fig. 1) was previously exposed in (Horodincă, 2020).

A trajectory T_i of a point P_i^{β} placed on SSGR (*i* is constant, β is variable) is a roulette-type curve. The internal envelope bordered by all trajectories T_i is also an approximation of 2D SGP.

Even though the 2D SGP generating by rolling with SSGR is privileged in this paper, we should mention that some researchers (Luo, 2008; Si *et al.* 2020) propose that the 2D SGP (as cosine gear profile in their works) is not generated by rolling with SSGR, but directly as a closed 2D sine circular profile (2D SCP) described in a fixed CCS *xOy* as an adaptation from (Si *et al*., 2020) by:

$$x = x_c + [R_p + h_a \sin(Z\varphi)]\cos(\varphi) \quad (4)$$

$$y = y_c + [R_p + h_a \sin(Z\varphi)]\sin(\varphi) \quad (5)$$

The same 2D SCP is generated if the datum (pitch) line of SSGR from Eq. (1) is wrapped around the pitch circle. Suppose that a current value of a parameter φ (the same from Eqs. (4), (5)) is defined as $\varphi = x_1(P_{i1})/R_p$ from which it follows that $x_1(P_{i1}) = \varphi R_p = \varphi mZ/2$. During wrapping process there is a rotary segment having one fixed endpoint in pitch circle origin, with φ as angular current position (here related to a vertical line passing through pitch circle origin). The other endpoint describes the 2D SCP. The length R_L of this rotary segment is variable, expressed as the addition between the pitch radius R_p and $y_1(P_{i1})$ from Eq. (1), so $R_L = R_p + y_1(P_{i1})$. In Eq. (1) $x_1(P_{i1})$ is replaced by $\varphi mZ/2$ as

was shown above. The coordinates x, y, of a current point placed on 2D SCP are evidently described as $x=R_L\cos(\varphi)$ and $y=R_L\sin(\varphi)$ and consequently as:

$$x = x_c + [R_p + h_a \sin(\frac{2}{m}\frac{\varphi mZ}{2})]\cos(\varphi) = x_c + [R_p + h_a \sin(Z\varphi)]\cos(\varphi) \quad (6)$$

$$y = y_c + [R_p + h_a \sin(\frac{2}{m}\frac{\varphi mZ}{2})]\sin(\varphi) = y_c + [R_p + h_a \sin(Z\varphi)]\sin(\varphi) \quad (7)$$

As expected, Eqs. (6), (7) are identical with Eqs. (4), (5). Nevertheless, we should mention that the 2D SCP is not perfect identical with 2D SGP (as this paper will prove later on). Two toothed wheel having 2D SCP (and *Z, Z'* number of teeth) with the same module m and addendum h_a doesn't mesh properly together, the gearing laws (Dooner, 2002) are not accomplished because the profiles were not generated by rolling (as 2D SGP it is). However, in order to have a perfectly matched gear, the 2D SCP from a toothed wheel should be mandatory transferred to the conjugate toothed wheel by rolling.

3. Simulation Results

All the simulations from this paper were done in Matlab. A first simulation result on 2D SGP generated by SSGR rolling (for Z=20, m=1mm, h_a=1mm, c_h=1) is exposed in Fig. 2, focused on the area of a single tooth.

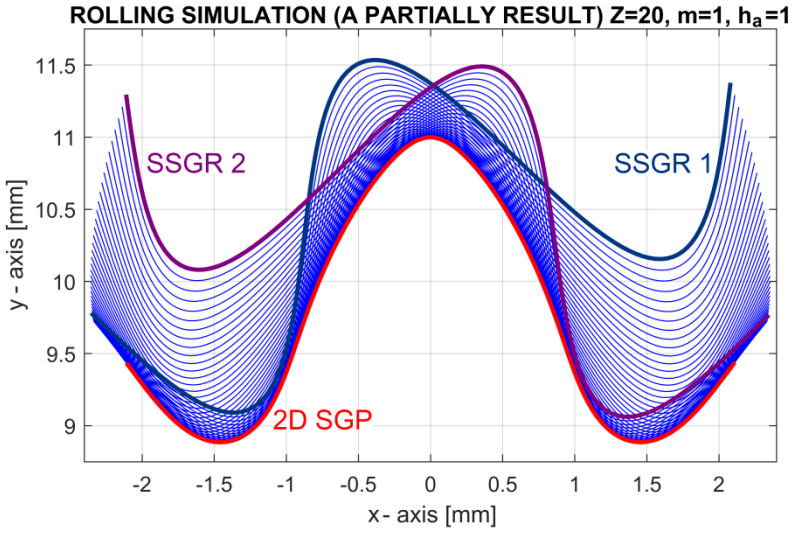

Fig. 2 – Some successive positions of SSGR during a partially simulation definition of 2D SGP by rolling.

Here 500 different equidistant positions of SSGR and 1000 positions of rotary ray (involved in 2D SGP detection) were used (for a completely rolling). The SSGR rolls in clockwise direction, between two extreme positions SSGR 1 and SSGR2.

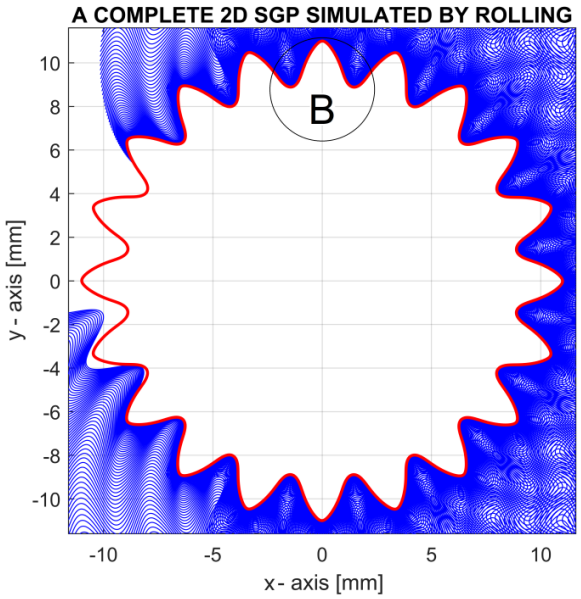

Fig. 3 – A completely 2D SGP simulation by rolling (Z=20, m=1mm, h_a=1mm, c_h=1).

The complete 2D SGP simulation by rolling is described in Fig. 3. A detail of B area is described in Fig. 4. The 2D SGP occurs as internal envelope bordered by all SSGR positions during a complete rolling.

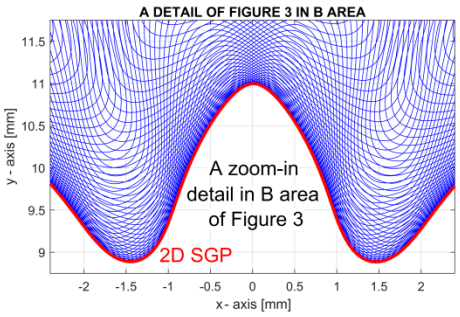

Fig. 4 – A 2D SGP as envelope bordered by SSGR positions.

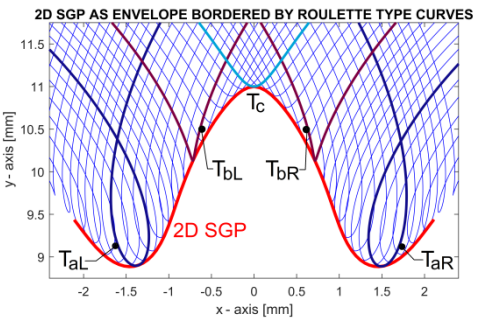

Fig. 5 – A 2D SGP as envelope bordered by roulette type curves (trajectories T_i).

Fig. 5 shows that the 2D SGP can be described also as internal envelope bordered by roulette-type curves (trajectories T_i described by all the point

placed on SSGR, some of them depicted on Fig. 5), a subject already discussed before in (Horodincă, 2020). All these trajectories are tangent to 2D SGP. There are three kinds of roulette-type curves highlighted in Fig. 5: T_{aL} and T_{aR} with returning lobe, T_{bL} and T_{bR} with returning point and T_c with returning arc. Here T_{bL} and T_{bR} curves are involutes, as being generated by points placed on SSGR and datum line (this line rolls around pitch circle which works as base circle).

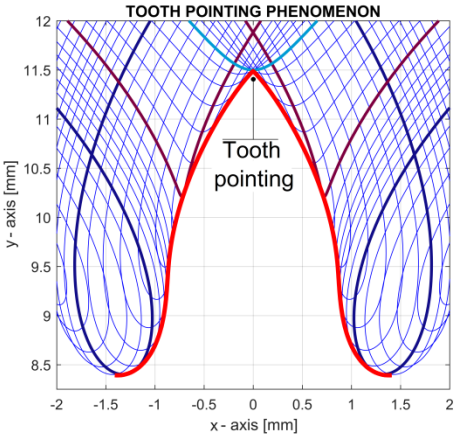

Fig. 6 – Tooth pointing phenomenon on 2D SGP (Z=20, m=1mm, c_h=1.5).

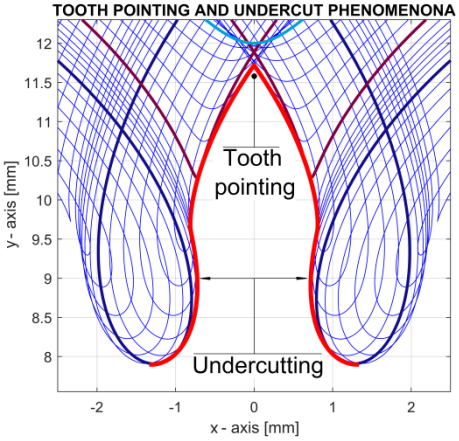

Fig. 7 – Tooth pointing and undercutting phenomena (Z=20, m=1mm, c_h=2).

A critical issue in 2D SGP simulation is the value of addendum h_a or more precisely the value of proportionality factor c_h from $h_a=c_hm$ relationship. A simulation of 2D SGP in similar conditions with Fig. 5 except the value of c_h (c_h=1.5, h_a=1.5m) proves (Fig. 6) that for high addendum (and small number of teeth Z) the tooth tip becomes sharp, a tooth pointing phenomenon occurs. If the factor c_h is increased more (c_h=2 in Fig. 7) apart from pointing occurs supplementary the undercutting phenomenon. However in practice, by similitude with involute gears, these high values of c_h factor (c_h>1) are not used.

The irregular distribution of curves T_i from Figs. 5 and 6 (compared with Fig. 4), can be an indicator of sliding between SSGR and 2D SGP during rolling.

The first major advantage of 2D SGP as against 2D involute gear profile (2D IGP) is graphically depicted in Fig. 8. Here both profiles are drawn, for the same number of teeth (Z=12), module (m=1mm) and addendum (h_a=1mm, equal with dedendum). The simulation of 2D IGP was done accordingly with a previous work (Horodincă, 2020). Here it is obvious the appearance of a well-known undercutting phenomenon on 2D IGP while on 2D SGP this undesired phenomenon doesn't occurs.

A second major advantage of 2D SGP as against 2D IGP is graphically depicted in Fig. 9, also both profile drawn for the same number of teeth (Z=30),

module (m=1mm) and addendum/dedendum (h_a=1mm). Here it is obvious that on 2D SGP the tooth thickness in the root area is bigger than 2D IGP tooth thickness. This means a lower bending stress on 2D SGP for the same loading. 2D SGP accept a higher loading for the same bending stress. Also, as a positive feature, because the top land of 2D GSP is rounded the edge effect in gearing disappears.

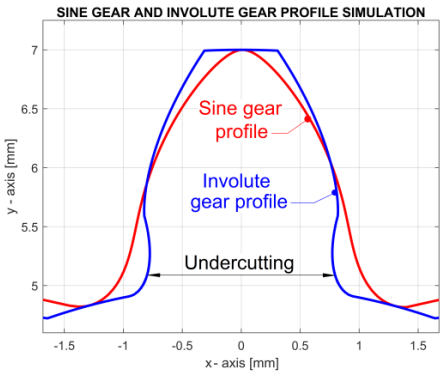

Fig. 8 – Sine and involute gear profiles simulation (Z=12, m=1mm, c_h=1, addendum equal with dedendum, 1mm).

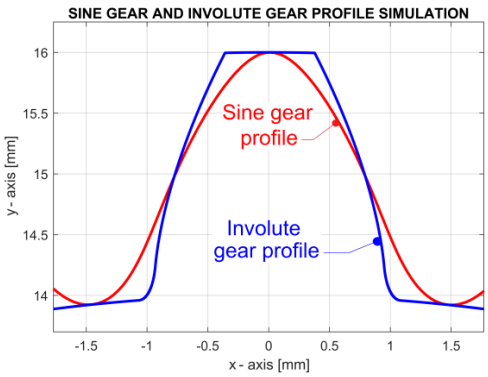

Fig. 9 – Sine and involute gear profiles simulation (Z=30, m=1mm, c_h=1, addendum equal with dedendum, 1mm).

However, because the 2D SGP have a smaller tooth thickness than 2D IGP in the tip circle area, is expected that the contact ratio for this type of gear decreases. This is a negative feature for external gears but is positive for internal gears because it helps avoiding the tip tooth interference (Si *et al*., 2020).

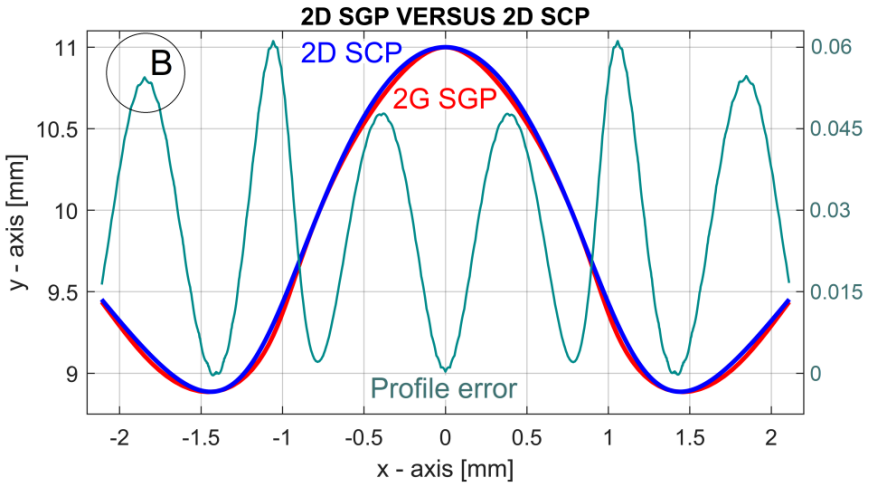

Fig. 10 – 2D SGP *versus* 2D SCP (Z=20, m=1mm, c_h=1).

A graphical description of a part of 2D SGP (revealed in Figs. 4 and 5) and a part of 2D SCP (calculated using Eqs. (4) and (5)) both for Z=20, m=1mm, h_a=1mm, (c_h=1) is done in Fig. 10. As already was said, it is obvious that these two profiles doesn't fit perfectly. The dissimilarity between these profiles is also described on Fig. 10 as profile error, or the evolution of difference between the ordinates of points placed on 2D SCP and the ordinates of points placed on 2D SGP as well.

The difference is permanently positive, as expected, it has a left-right symmetrical periodical shape. Some very small variations of the profile error (*e.g.* in B area) are related by incremental definition of 2D SGP (due to incremental positions of SSGR).

A high quality and precision of gearing is obtained of course only using 2D GSP. Only for some unpretentious applications this profile can be replaced with 2D SCP.

The 2D SGP is suitable for spur and helical external and internal gears.

Fig. 11 presents a simulation of 2D SGP for an internal gear (20/25 gear ratio), both toothed wheels having the same SSGR (m=1mm, c_h=1).

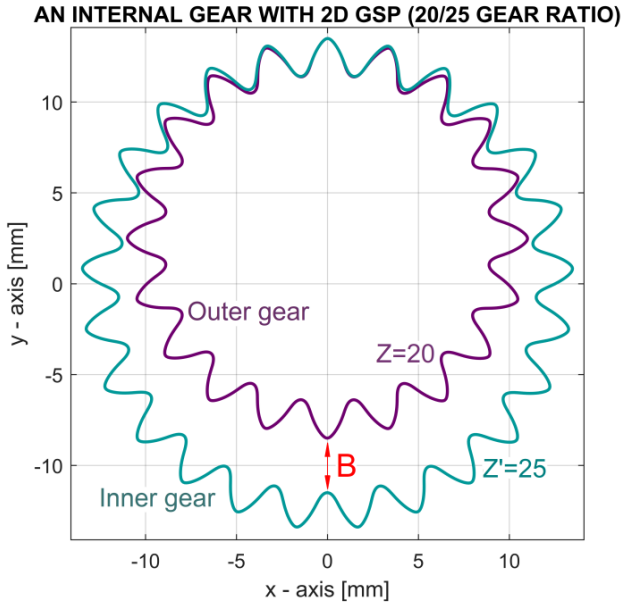

Fig. 11 – 2D SGP of an internal gear (Z=20, Z'=25, m=1mm, c_h=1).

One of two toothed wheels involved in this internal gear (*e.g.* outer gear) can have 2D SCP but for a precise gearing, the other toothed wheel (inner gear) should mandatory have a profile generated by rolling (during rolling a wheel works as a tool for the other, similarly with a gear shaper process).

Because an internal gear with 2D SGP doesn't need clearance, it is suitable for pumps. For some applications with internal gears is desirable to have a small difference of teeth numbers (*e.g.* in planetary gears, Si *et al.*, 2020), sometimes at the lowest limit with Z'-Z=1. This odd lowest limit implies to solve a relatively difficult problem: the tip tooth interference in the circle diametrically opposite point to the pitch point (see B area in Fig. 11, on an internal gear having also an odd difference Z'-Z=5).

An internal gear, avoids apparently the interference in this point if Z'-Z=2, (the outer gear having permanently a tooth aligned with a space on the inner gear) as it is proved in Fig. 12, but there are other regions (highlighted with red bullet points) where the interference take places.

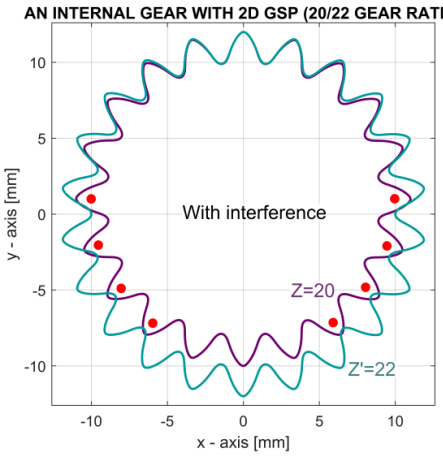

Fig. 12 – 2D SGP of an internal gear (Z=20, Z'=22, m=1mm, c_h=1) with tooth tip interferences.

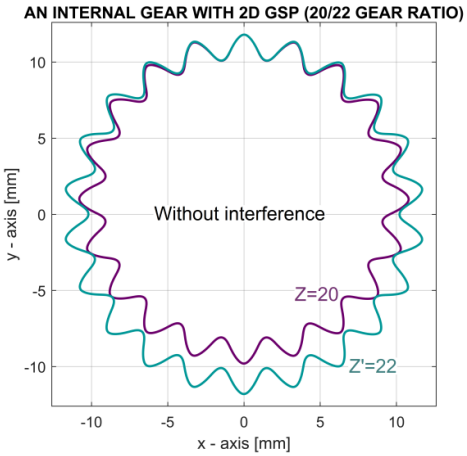

Fig. 13 – 2D SGP of an internal gear (Z=20, Z'=22, m=1mm, c_h=0.8) without tooth tip interferences.

There is a simple way to eliminate this interference as Fig. 13 proves: to reduce the tooth addendum $h_a=c_h \cdot m$ or to reduce the value of c_h factor as well on both toothed wheels until the interference disappears. Thus, in Fig. 13 c_h=0.8, in contrast with Fig. 12, where c_h=1. An internal gear having Z'-Z=2 is currently used in harmonic drives. Here because the outer gear (or the flexspline as well) is deformable (having an almost elliptical cross section) it is possible to avoid the tip tooth interference with c_h>0.8. Taken into account the other advantages of 2G SGP probably is a good option to use this profile in a harmonic drive.

It is possible to generate the 2D SGP for an internal gear having Z'-Z=1 without interference based on a study depicted in Fig. 14 (Z'=21, Z=20, m=1mm, $h_a=1 \cdot m$, c_h=1). In area B, the tip of outer gear is placed on the pitch circle of the inner gear and the tip of inner gear is placed on the pitch circle of the outer gear (because the addendum is equal with dedendum on both wheels),

so it is easy to observe that the interference can be avoided at the limit by halving the addendum h_a (from $h_a=1\cdot m$ to $h_a=0.5\cdot m$) or the factor c_h as well (from $c_h=1$ to $c_h=0.5$) during profile generation by rolling of both toothed wheel.

The efficiency of this decision is fully confirmed by simulation, as Fig. 15 proves, the interference disappears; now the gear should work properly.

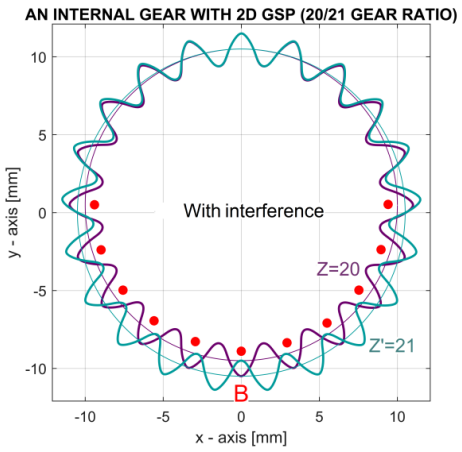

Fig. 14 – 2D SGP of an internal gear (Z=20, Z'=21, m=1mm, c_h=1) with tooth tip interferences.

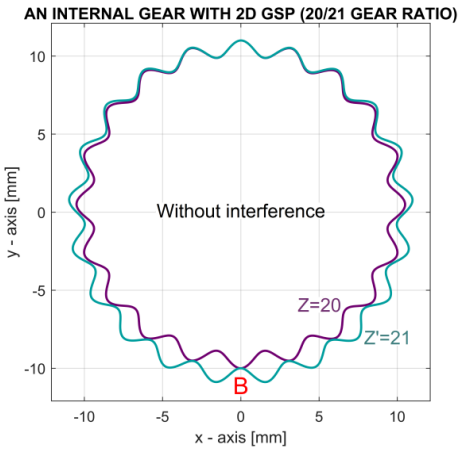

Fig. 15 – 2D SGP of an internal gear (Z=20, Z'=21, m=1mm, c_h=0.5) without interferences.

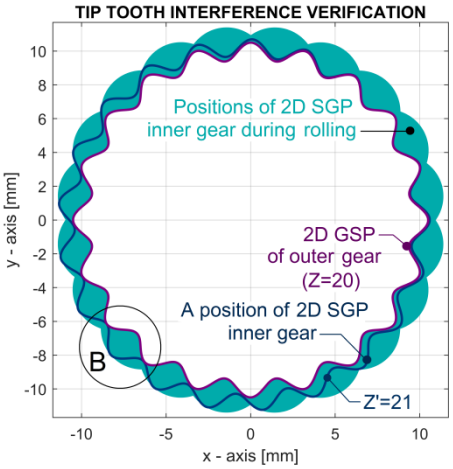

Fig. 16 – Tip tooth interference verification by rolling (on internal gear).

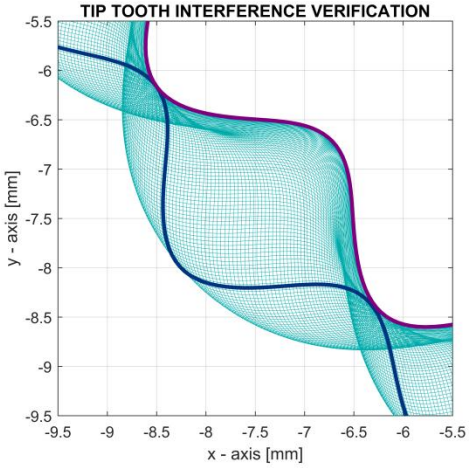

Fig. 17 – A detail in B area of Fig. 16.

With c_h=0.5 in B area on Fig. 15 there is a temporary sliding contact between the teeth tips. If it is necessary to avoid this contact, c_h should be reduced a little more.

There is a simple way to verify that an internal gear with Z'-Z=1 and c_h=0.5 works properly (no matter the values of Z', Z and m), without tip tooth interference: by rolling the movable pitch circle of inner gear together with Z' 2D SGP around the fixed pitch circle of outer gear Z. If there is no any tip tooth interference, then the inner envelope bordered by the 2D SGP positions of inner gear (Z') should be exactly the 2D SGP of outer gear (Z). This is confirmed in the graphical result of simulation from Fig. 16 using the 2D profiles depicted in Fig. 15 (Z=20, Z'=21, m=1mm, c_h=0.5). Fig. 17 depicts a detail of Fig. 16 in B area. The positions of inner gear profile are strictly bordered by outer gear profile. This happens certainly everywhere on the 2D GSP of outer gear.

Similarly, by rolling, can be clearly indicated the interference for the internal gear whose profiles are depicted in Fig. 12 (Z=20, Z'=22, m=1mm, c_h=1), as Fig. 18 proves. In contrast to Fig. 17 the positions of inner gear profile are not totally internally bordered by outer gear profile. Certainly this internal gear doesn't work.

Also by rolling simulation, Fig. 19 indicated the lack of interference for the internal gear with the profiles depicted in Fig. 13 (Z=20, Z'=22, m=1mm, c_h=0.8). This internal gear works properly.

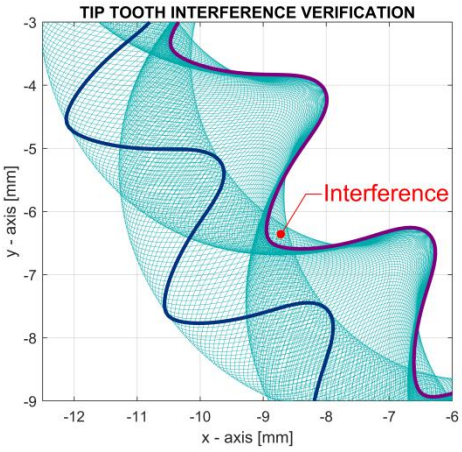

Fig. 18 – Tip tooth interference proved by rolling for the internal gear from Fig. 12 (Z=20, Z'=22, m=1mm, c_h=1).

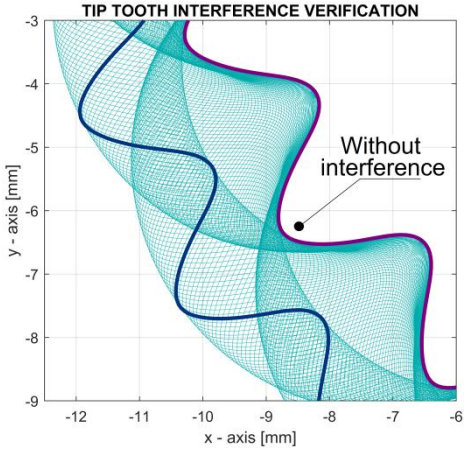

Fig. 19 – The lack of interference proved by rolling for the internal gear from Fig. 13 (Z=20, Z'=22, m=1mm, c_h=0.8).

If we return back to the internal gear with Z'-Z=1 and c_h=1 (with a study of interference done in Fig. 14), we should mention that the tip tooth interference can be avoided also by reducing (increasing) the tip radius of outer (inner) gear (*e.g.* by a turning process on each gear blank previously the gearing process) until the interference completely disappears. Of course the easiest way is to decide the values of these profiles corrections (values of tip radii) by computer aided simulation before manufacturing.

The 2D SGP of internal gear with modified tip radii are depicted in Fig. 20. The tip radius of outer gear is reduced from $m \cdot Z/2+1m$ to $m \cdot Z/2+0.23m$ while the tip radius of inner gear is increased from $m \cdot Z/2-1m$ to $m \cdot Z/2-0.23m$, or the addendum is diminished from 1m to 0.23m on both gears (inner and outer).

The lack of tip tooth interference is proved by rolling in Fig. 21. Unfortunately, on Fig. 20 is evidently that by decreasing (increasing) of tip radii the total contact surface is drastically reduced (and the loading capacity as well) compared with an internal gear having c_h=0.5 and uncorrected 2D SGP (Fig. 15). This inconvenient is seriously worsened by the apparition of the undesired edge effect of the teeth tips.

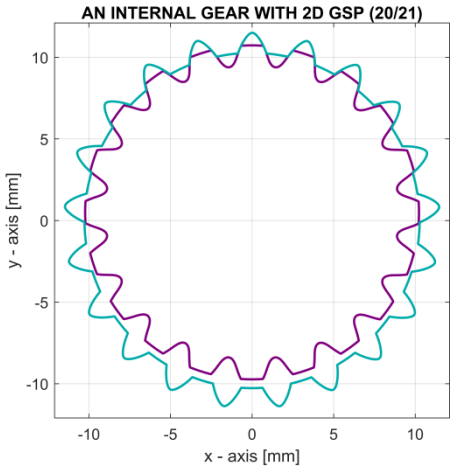

Fig. 20 – The avoidance of interference of the internal gear with 2D SGP from Fig. 14 by tip radii corrections.

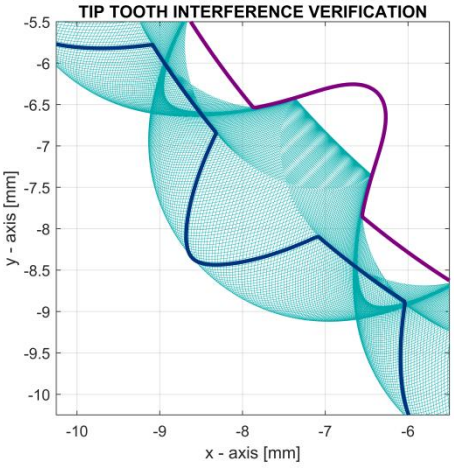

Fig. 21 – The lack of interference proved by rolling for the internal gear from Fig. 20.

These studies proves that the best decision for an internal gear with Z'-Z=1 in order to avoid tip tooth interference is to use a value c_h=0.5 in the definition of tooth addendum (dedendum). This type of internal gear can be used inside a speed reducer working similarly with a cycloidal drive (here with-$(Z'-Z)/Z=-1/Z$=-1/20 speed ratio). A prototype of this internal gear manufactured by 3D printing confirms that it works properly, including the behaviour as a cycloidal drive.

4. Conclusions

The computer aided simulation of a cross section 2D sine gear profile (2D SGP) used on spur (or helical) gears is the main purpose of this paper. The simulation is based on the rolling of a movable sine shape generating rack (SSGR) on a fixed pitch circle. A previous developed mathematical model of

rolling for involute profiles (slightly adapted here for 2D GSP) and a 2D profile detection method (Horodincă, 2020) were used in this paper.

The inner envelope bordered by as many as possible angular uniformly distributed positions of SSGR during a completely rolling defines the best approximation of a 2D SGP. Each SSGR position and finally the 2D SGP are described by the Cartesian coordinates of a succession of extremely closed equidistant points, with line segments between.

The rolling simulation method of 2D SGP proposed in this paper (using Matlab) helps a better understanding of the features and the behavior of this type of gear profile, proved in some particular cases (*e.g*. the study of undercutting and tooth pointing phenomenon, tooth thickness in the root area, a comparison with a possible substitution of sine gear profile with a sine circular profile, etc.).

A consistent part of this paper was reserved to a study related with the gearing features of internal gears with 2D SGP having small teeth number differences (used frequently in planetary reducers). Especially the tip tooth interference and some solutions to detect and to avoid this undesired phenomenon were revealed by simulation. It was proved that the 2D GSP is suitable for internal gears with smallest possible teeth number difference (1) if the addendum (and dedendum as well) is 0.5m on both gears.

The 2D SGP are fully available for computer aided design of 3D model of spur (or helical gears) and additive manufacturing (3D printing) and for manufacturing by cutting processes (2D contouring on CNC milling machines) or equivalent processes (laser, wire electrical discharge machining, water jet cutting, etc.).

Some other research possibilities based on simulation are available for a future research (*e.g*. computer aided automatically tip tooth interference detection for internal gears, undercutting and tooth pointing detection, etc.)

A simulation of bevel spiral gears and hypoid gears by 3D rolling will be considered for a future work.

REFERENCES

Alipiev O., Antonov S., Grozeva T., *Generalized Model of Undercutting of Involute Spur Gears Generated by Rack-Cutters*, Mechanism and Machine Theory, **64**, 39-52 (2013).

Dooner D.B., *On the Three Laws of Gearing*, Journal of Mechanical Design, **124**, *4* 744-744 (2002).

Horodincă M., *An Approach on Simulation of Involute Tooth Profile Used on Cylindrical Gears*, Bul. Inst. Polit. Iaşi, s. Machine Construction, **(66)70**, *2*, 21-36 (in press) (2020).

Hrytsay I., Stupnytskyy V., *Analysis of the Involute and Sinusoidal Gears by the Operating Parameters and a New Method of its Cutting*. In: Ivanov V. *et al.*

(Eds.) Advances in Design, Simulation and Manufacturing II. DSMIE 2019, Lecture Notes in Mechanical Engineering, Springer, Cham. (2020) https://doi.org/10.1007/978-3-030-22365-6_11.

Hu H.R., Wang J., *Experimental Study of Flow Rate and Its Ripple of a Cosine Gear Pump*, Applied Mechanics and Materials, Trans Tech Publications Ltd., **220–223,** 661-664 (2012).

Laczik B., Zentay P., Horvath R., *A New Approach for Designing Gear Profiles Using Closed Complex Equations*, Acta Polytechnica Hungarica, **11**, *6*, 159-172 (2014).

Lee C.K., *A Comparative Study Between a Pair of Cosine Gears and a Pair of Involute Gears: Contact Stress, Root Fillet Stress, and Contact Ratio*, APETC 2017, 2017 Asia-Pacific Engineering and Technology Conference, Kuala Lumpur, Malaysia, 25–26 May 2017, 354-361 (2017).

Lee C.K., *The Mathematical Model and a Case Study of the Cosine Face Gear Drive that has a Predesigned Fourth Order Function of Transmission Errors and a Localized Bearing Contact*, Advances in Mechanical Engineering, **11**, *2*, 1-20 (2019).

Luo S., Wub Y., Wang J., *The Generation Principle and Mathematical Models of a Novel Cosine Gear Drive*, Mechanism and Machine Theory, **43**, 1543-1556 (2008).

Si C., Chen Z., Zhang H., Zhang Y., Cui C., *Cosine Gear Planetary Transmission with Small Teeth Number Difference*, International Conference on Energy, Power and Mechanical Engineering (EPME 2019), IOP Conf. Series: Materials Science and Engineering,**793** 012034 (2020).

Tkach P., Nosko P., Bashta O., Tsybrii Y., Revyakina O., Boyko G., *Comparison of Sinusoidal and Involute Spur Gears by Meshing Characteristics*, Proceedings of Odessa Polytechnic, Machine Building Engineering, Ukraine, **1**, *57*, 41-51 (2019).

Zheng F., Hua L., Han X., Chen D., *Generation of Noncircular Bevel Gears With Free-Form Tooth Profile and Curvilinear Tooth Lengthwise*, Journal of Mechanical Design, Transactions of the ASME, **138**, 064501-2- 064501-7 (2016).

Wadagaonkar S., Shinde S., *Cosine Gear Stress Analysis with Experimental Validation, and Comparison with Involute Gear*, International Journal of Innovative Science, Engineering & Technology, **2**, *3*, 438-443 (2015).

Wildhaber E., *Gear Tooth Shape*, United States Patent Office, 3251236 (1966).

https://en.wikipedia.org/wiki/List_of_gear_nomenclature

UN STUDIU AL PROCESULUI DE GENERARE A PROFILELOR SINUSOIDALE UTILIZATE PE ROȚILE DINȚATE CILINDRICE

(Rezumat)

Lucrarea prezintă o serie de abordări teoretice legate de simularea profilelor 2D ale roților dințate cilindrice cu profile sinus (în secțiune transversală). Comparativ cu profilele evolventice, cele cu profile sinus sunt mai avantajoase deoarece prezintă

alunecări mai reduse între flancuri, au capacitate de încărcare mai mare și asigură o funcționare mai silențioasă. Asemănător cu metoda de generare a profilelor evolventice pe flancurile roților dințate, profilele sinus sunt obținute prin rularea unei cremaliere generatoare cu profil sinusoidal peste un cerc de rostogolire fix. Anvelopa interioară mărginită de pozițiile cremalierei generatoare în timpul rulării descrie profilul 2D al danturii cu profil sinus. Principalele realizări ale acestei lucrări sunt legate de simularea rulării și detecția descrierii 2D a profilelor sinus în diferite situații. Este cercetată de asemeni influența formei cremalierei generatoare (înălțimea dintelui) asupra profilului generat.